

See discussions, stats, and author profiles for this publication at: <https://www.researchgate.net/publication/258441642>

Comparison of the Mechanism of Borane, Silane, and Beryllium Hydride Ring Insertion into N-Heterocyclic Carbene C–N Bonds: A Computational Study

ARTICLE *in* ORGANOMETALLICS · OCTOBER 2013

Impact Factor: 4.13 · DOI: 10.1021/om400800d

CITATIONS

23

READS

12

3 AUTHORS:



[Kalon Jake Iversen](#)

La Trobe University

10 PUBLICATIONS 69 CITATIONS

SEE PROFILE



[David J D Wilson](#)

La Trobe University

69 PUBLICATIONS 633 CITATIONS

SEE PROFILE



[Jason L Dutton](#)

La Trobe University

50 PUBLICATIONS 734 CITATIONS

SEE PROFILE

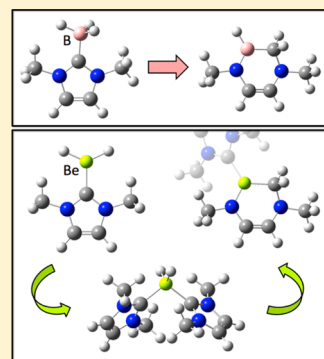
Comparison of the Mechanism of Borane, Silane, and Beryllium Hydride Ring Insertion into N-Heterocyclic Carbene C–N Bonds: A Computational Study

Kalon J. Iversen, David J. D. Wilson,* and Jason L. Dutton*

Department of Chemistry, La Trobe Institute for Molecular Science, La Trobe University, Melbourne, Victoria 3086, Australia

S Supporting Information

ABSTRACT: A computational investigation has been carried out on the mechanism and energetics of the experimentally observed insertion/ring expansion of N-heterocyclic carbenes (NHCs) by boranes (H_2BNHR , BH_3 ; $R = Me, Ph$) and beryllium hydrides (BeH_2) in comparison with silanes (SiH_2R_2 ; $R = Me, Ph$). The results suggest that the ring insertion mechanisms are similar for boranes, beryllium hydrides, and silanes. The principal mechanism components are (1) hydrogen atom migration to the carbene carbon, (2) C–N bond expansion of the NHC with insertion of the main-group hydride into the ring, and (3) migration of a second hydrogen atom to the carbene carbon. The synthetically important NHC· BH_3 adduct is also predicted to be thermodynamically unstable with respect to this transformation but is kinetically stabilized with a high barrier to the first hydrogen atom migration. The BeH_2 insertion product provides a rare example of a Be–N π interaction.



INTRODUCTION

The synthesis of N-heterocyclic carbene (NHC) stabilized element hydrides is a current topic of interest in main-group chemistry.^{1–9} Three recent synthetic papers have described a ring expansion of NHCs in the presence of main-group hydride species.^{10–12} These include silanes, boranes, and beryllium hydrides as depicted in reactions 1–4 in Scheme 1, respectively. While NHCs and other carbenes have been reported to activate several different types of substrates,^{13–15} ring expansion of the NHCs themselves is a new form of reactivity. Such a ring expansion reaction, as indicated by Hill, Radius, and Rivard in their respective synthetic papers,^{10–12} has implications in possible degradation pathways for NHCs in catalytic systems, particularly if metal hydrides are involved. Guided by the mechanism proposed by Radius and co-workers in their synthetic paper,¹² we have conducted an initial theoretical study of the silane mediated expansion of NHCs (reaction 1).¹⁶ The largest stepwise barrier for the reaction is calculated to be 113 kJ/mol (MP2/def2-TZVP//M06-2X/6-31G(d)), corresponding to migration of the first hydrogen atom from the silane to the carbene carbon of the NHC ring. Such a barrier height is consistent with the reported synthetic conditions (refluxing toluene, multiple days). The overall driving force for the reaction is proposed to be the formation of C–H bonds at the expense of Si–H bonds, which is calculated to be energetically favorable. Investigation of the analogous process with chlorosilanes, for which stable adducts are known,^{17–20} predicted the reaction to be unfavorable, as the energy required to form C–Cl bonds is greater (maximum barrier height is 182 kJ/mol and overall reaction is endergonic by 125 kJ/mol).

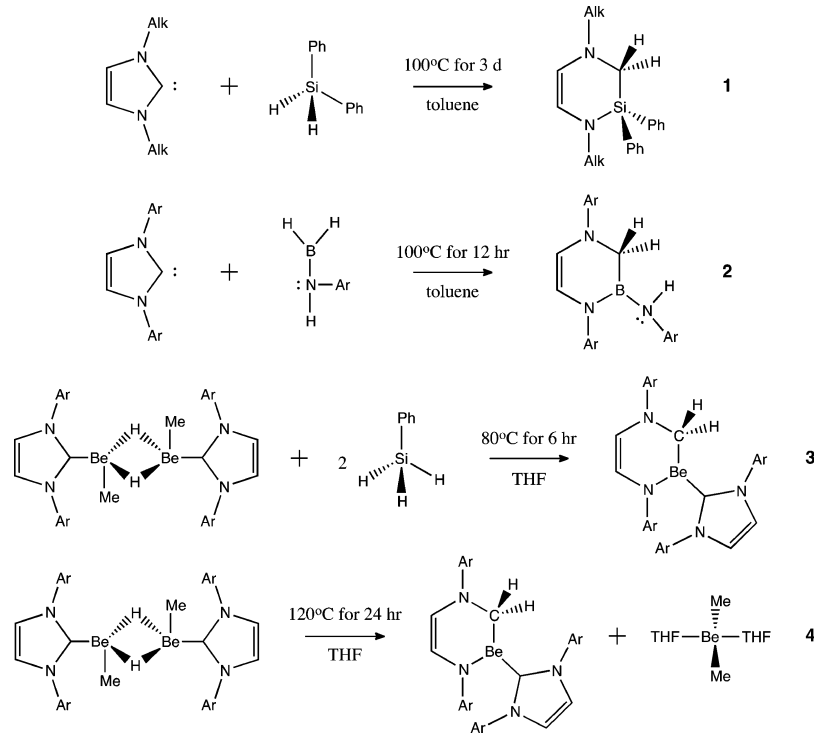
Here we outline a theoretical investigation of the mechanism and energetics of boron- and beryllium-mediated NHC ring expansion using the species outlined in the synthetic papers. Furthermore, we have explored the (unobserved) expansion reaction for the synthetically important $R_2NHC\cdot BH_3$ family of adducts,^{21–31} to ascertain whether this class of species is stable with respect to insertion/ring expansion.

COMPUTATIONAL METHODS

All calculations were carried out within Gaussian 09.³² Geometries of all structures were optimized using the M06-2X density functional theory (DFT) method,³³ using default convergence criteria. Other DFT functionals, including B3LYP³⁴ and PBE1PBE,³⁵ produced similar geometries and so are not included. Structures were optimized separately with 6-31G(d), def2-SVP, and def2-TZVP basis sets,^{36,37} unless noted, only def2-TZVP basis set results are presented since the geometries were found to be largely independent of the basis set. The larger Dipp₂NHC complexes were optimized only with the 6-31G(d) basis set. Geometry optimization of transition states employed the quadratic synchronous transit (QST) approach.³⁸ Intrinsic reaction coordinate calculations were carried out to ensure transition states connected the appropriate local minima. Stationary points were characterized as minima or transition states by calculating the Hessian matrix analytically at the same level of theory. All structures labeled as minima exhibit no imaginary frequencies; transition states exhibit one imaginary frequency. Thermodynamic corrections were taken from these calculations (standard state of $T = 298.15$ K and $p = 1$ atm). Cartesian coordinates of all optimized structures are included in the Supporting Information.

Received: August 9, 2013

Published: October 10, 2013

Scheme 1. Reported Reactions Where a Main-Group Hydride Inserts into the C–N Bond of R_2NHC^a 

^aAbbreviations: Ar = Dipp = 2,6-diisopropylphenyl; Alk = Me, ⁱPr, ⁿPr. Reactions: (1) silane,¹² (2) borane,¹⁰ and (3, 4) beryllium hydride.¹¹ Formal charges are omitted.

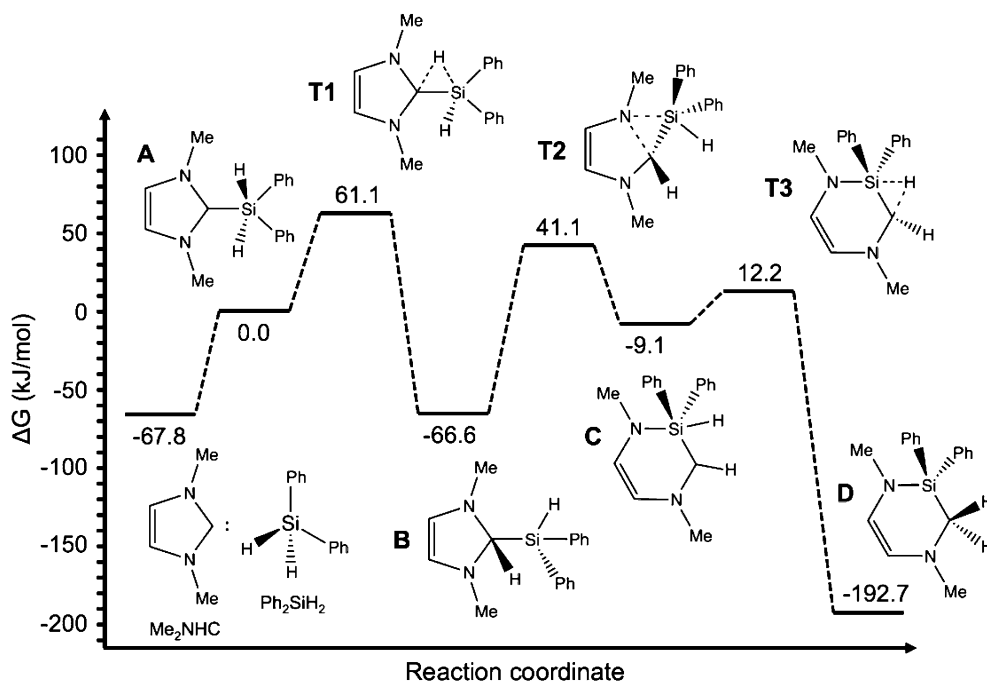


Figure 1. Free energy profile (ΔG , kJ/mol) for reaction 1 from Scheme 1 for $R = \text{Me}$ in R_2NHC calculated with SCS-MP2/def2-TZVP//M06-2X/def2-TZVP. Formal charges are omitted. Minima are denoted A–D, and transition states are denoted T_n ($n = 1–3$).

Single-point MP2/def2-TZVP energies (including SCS-MP2³⁹ and SOS-MP2⁴⁰) were calculated using the M06-2X/def2-TZVP optimized geometries. MP2 energies in the tables are presented as $\Delta G_{298\text{ K}}$ values, which combine the MP2/def2-TZVP electronic energy and M06-2X/def2-TZVP thermochemical correction. MP2 energies calculated at M06-2X/6-31G(d) optimized geometries produced relative reaction energies within 6 kJ/mol of MP2 energies calculated

at M06-2X/def2-TZVP optimized geometries. The effect of solvent on geometries and reaction energetics was investigated for several reactions, using the integral equation formulation of the polarizable continuum model (IEFPCM)^{41–43} with either THF or toluene solvent parameters (as employed by Hill¹¹ and Rivard,¹⁰ respectively). Only minor differences were noted for optimized geometries in solvent-phase calculations, with relative MP2 reaction energies within 8 kJ/

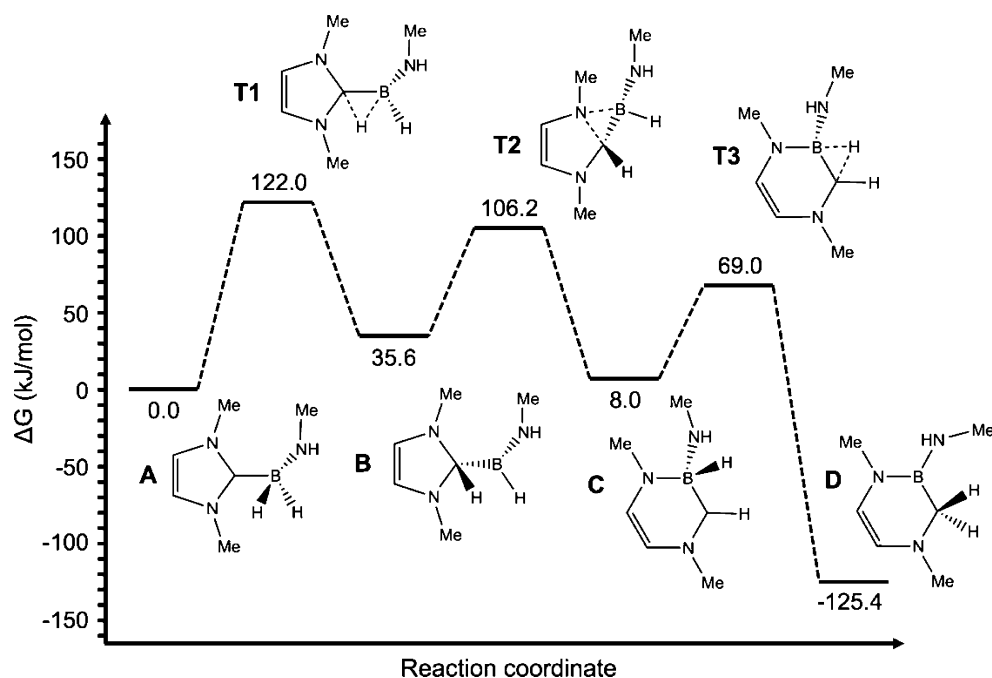


Figure 2. Free energy profile (ΔG , kJ/mol) for reaction 2 from Scheme 1 for $R = \text{Me}$ in $R_2\text{NHC}$ calculated with SCS-MP2/def2-TZVP//M06-2X/def2-TZVP. Formal charges are omitted. Minima are denoted A–D, and transition states are denoted T_n ($n = 1–3$).

Table 1. SCS-MP2/def2-TZVP//M06-2X/def2-TZVP Calculated Free Energies (ΔG , kJ/mol) for the Potential Energy Surface of the Reaction of $R_2\text{NHC}$ with Boranes to Form the Insertion Product D^a

| reactants | | ΔG of reaction | | | | | | | |
|-------------------------|--------------------------|------------------------|-----|----------|-------|----------|-------|-------|--------|
| | | reactants | A | T1 | B | T2 | C | T3 | D |
| Me_2NHC | BH_3 | 170.7 | 0.0 | 167.1 | 113.2 | 126.1 | 35.9 | 85.5 | −51.7 |
| Ph_2NHC | BH_3 | 150.2 | 0.0 | 149.3 | 78.4 | 86.5 | 10.3 | 50.6 | −85.9 |
| Me_2NHC | BH_2NHMe | 25.6 | 0.0 | 122.0 | 35.6 | 106.2 | 8.0 | 69.0 | −125.4 |
| Ph_2NHC | BH_2NHMe | 8.1 | 0.0 | 94.2 | −15.7 | 73.1 | −13.5 | 37.1 | −167.9 |
| Me_2NHC | BCl_3 | 135.8 | 0.0 | <i>b</i> | 229.3 | <i>b</i> | 117.8 | 189.0 | 170.0 |

^aEnergies are given relative to A. See Figures 2 and 3 for structures. ^bNo transition state located.

mol of the gas-phase MP2 results; therefore, only gas-phase results are presented. Basis set convergence was investigated with the $\text{NHC}\cdot\text{BH}_3$ system, with a variation of less than 4.1 kJ/mol between def2-TZVP and def2-QZVP calculated relative energies at the SCS-MP2 level of theory. Similar trends in basis set convergence may be expected for the other systems considered in this work.

RESULTS AND DISCUSSION

For the purpose of the following discussion, it is relevant to summarize the reaction profile of the silane analogue (Figure 1). For consistency with the Be/B results, we report SCS-MP2/def2-TZVP//M06-2X/def2-TZVP calculated free energies, which differ only slightly from the MP2/def2-TZVP//M06-2X/6-31G(d) results reported previously.¹⁶

Ring insertion into Me_2NHC by the silanes proceeds via the following four steps. The first step includes the formation of a fleeting Me_2NHC –silane adduct (A), which is 67.8 kJ/mol higher in energy (ΔG) than the free reactants (Me_2NHC and Ph_2SiH_2). The main feature of the adduct is that the hydrogen atoms are found in axial positions, perpendicular to the $\text{Si}\cdots\text{C}_{\text{NHC}}$ bond axis, which is ideally located for the subsequent H-migration step. Second, the migration of one hydrogen atom from the silane to the carbene carbon gives minimum B via transition state T1. The energy barrier for this reaction is 61.1

kJ/mol from the adduct A or 128.9 kJ/mol from the free reactants. Minimum B is 66.6 kJ/mol lower in energy than the adduct A. The third step is the insertion of the Si atom into the endocyclic C–N bond, giving minimum C via transition state T2. The energy barrier for this step is calculated to be 107.7 kJ/mol, while ring insertion (from B to C) is endergonic by 57.5 kJ/mol. The fourth step involves migration of the second hydrogen atom to the former NHC central carbon, giving the final product D via transition state T3. The energy barrier for this step was calculated to be 21.3 kJ/mol. The overall reaction to produce the final product D is favorable, being exergonic by 192.7 kJ/mol from adduct A and 124.9 kJ/mol from the free reactants.

The calculated pathway for the reaction of the silane with Me_2NHC , which is based on the proposal by Radius, is also consistent with their experimental kinetic data suggesting a bimolecular process.¹²

For the B/Be species considered in the present study, a primary difference from the silane– $R_2\text{NHC}$ adducts is that the starting borane– $R_2\text{NHC}$ and beryllium hydride– $R_2\text{NHC}$ adducts are lower in energy than the separated $R_2\text{NHC}$ and main-group hydride starting materials. Consequently, in this study the calculated reaction profiles are presented relative to

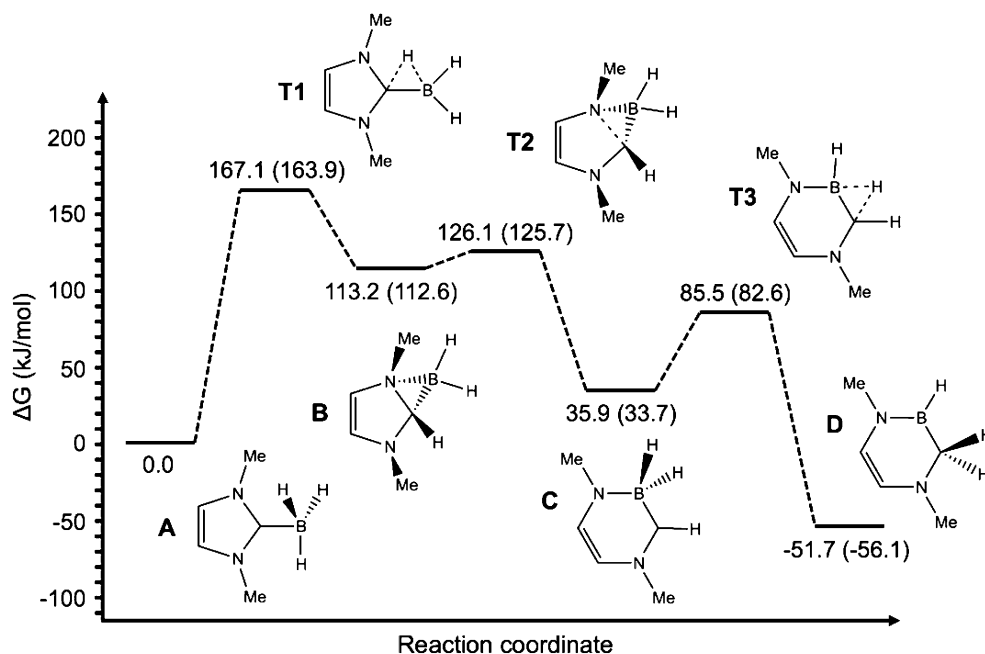


Figure 3. SCS-MP2/def2-TZVP//M06-2X/def2-TZVP calculated free energy reaction profile (ΔG , kJ/mol) for the insertion of BH_3 into the endocyclic C–N bond of Me_2NHC . SCS-MP2/def2-QZVP results are given in parentheses. Formal charges are omitted. Minima are denoted A–D, and transition states are denoted T n ($n = 1$ –3).

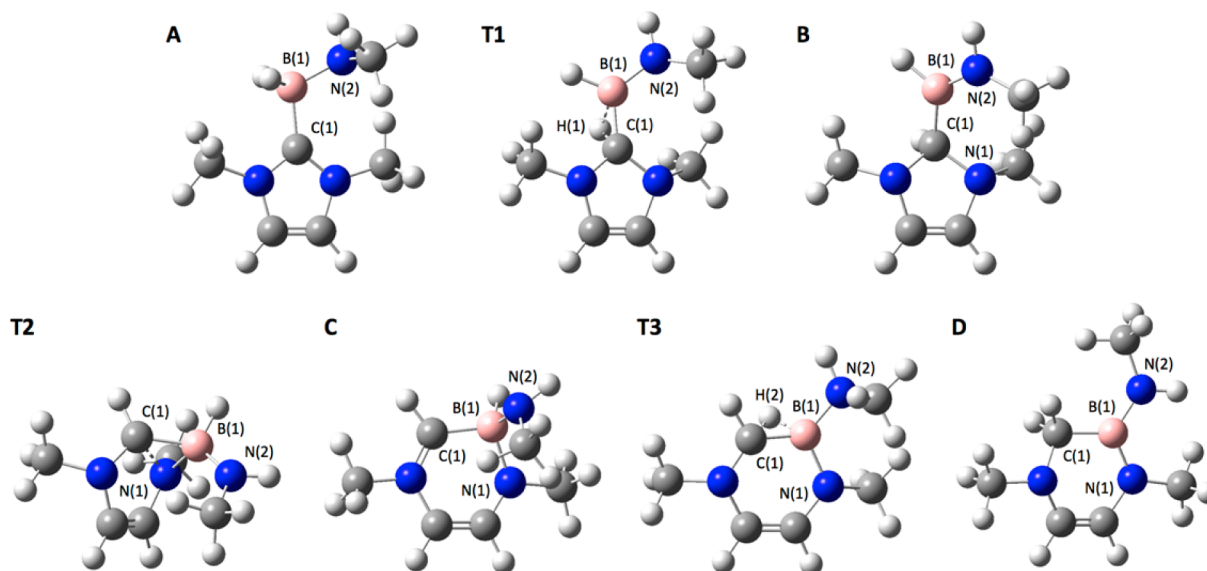


Figure 4. M06-2X/def2-TZVP optimized geometry of minima and transition states for insertion of boron into the endocyclic C–N NHC bond (reaction 2, Scheme 1).

the hydride– R_2NHC adducts rather than the separated main-group hydride and R_2NHC . For the silane reactions we found that the alkyl/aryl substitution pattern for the R groups on the silane ($\text{SiH}_n\text{Ph}_{4-n}$ and $\text{SiH}_n\text{Me}_{4-n}$; $n = 2, 3$) had relatively subtle effects on the calculated reaction energies. Replacement of methyl with phenyl groups on the silane caused the free energy of the reaction to become approximately 15 kJ/mol more negative per substitution, although the overall energy profile and mechanism of the reaction was not altered. In the present study of B/Be, we have considered both $\text{R} = \text{Me}$ and Ph substituents on the NHCs (R_2NHC).

Boranes. The experimental conditions under which the insertion/ring expansion was observed for boron (Scheme 1,

reaction 2) involved using the borane $\text{H}_2\text{BNH}(\text{Dipp})$ ($\text{Dipp} = 2,6\text{-diisopropylphenyl}$) with two hydrides bound to boron.¹⁰ Heating the Dipp_2NHC adduct of this borane in toluene at 100 °C for 12 h gave the insertion product in quantitative yield, which is similar to the conditions reported for the silane reaction. We modeled a pathway similar to that of the silane using the simplified borane H_2BNHMe , and indeed found an energy profile similar to that of the silane (Figure 2, Table 1). The largest barrier was calculated to be 122.0 and 94.2 kJ/mol for $\text{R} = \text{Me}$, Ph , respectively, which occurred for migration of the first hydrogen atom from the boron to the central carbene carbon (from A to T1). The finding that the first hydrogen atom migration is the rate-determining step is consistent with

Table 2. M06-2X/def2-TZVP Calculated Bond Distances (Å) and WBI Values (in Parentheses) for the Minima and Transition States for Insertion of Boron into the Endocyclic C–N NHC Bond (Reaction 2, Scheme 1)^a

| | bond distance, Å (WBI value) | | | | | | |
|-----------|------------------------------|--------------|--------------|--------------|--------------|--------------|--------------|
| | A | T1 | B | T2 | C | T3 | D |
| B(1)–C(1) | 1.630 (0.87) | 1.530 (1.02) | 1.592 (0.88) | 1.578 (0.86) | 1.618 (0.87) | 1.541 (1.04) | 1.593 (0.90) |
| B(1)–H(1) | 1.221 (0.94) | 1.503 (0.36) | | | | | |
| B(1)–H(2) | | | | | 1.213 (0.95) | 1.375 (0.55) | |
| B(1)–N(1) | | | 2.639 (0.01) | 1.651 (0.55) | 1.577 (0.70) | 1.503 (0.79) | 1.424 (0.97) |
| B(1)–N(2) | 1.522 (0.86) | 1.438 (1.00) | 1.387 (1.23) | 1.457 (0.96) | 1.507 (0.86) | 1.471 (0.91) | 1.413 (1.07) |
| C(1)–N(1) | | | 1.469 (0.97) | 1.651 (0.54) | | | |

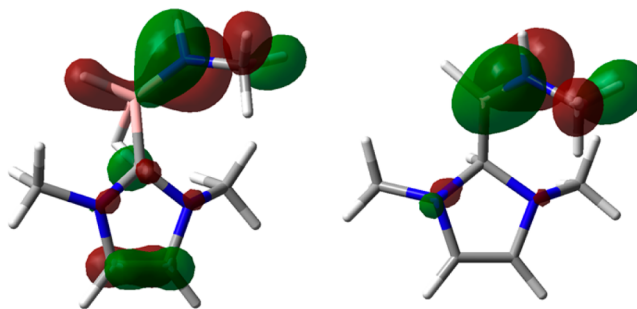
^aSee Figure 4 for atom labeling.

the silane case. The ΔG for the overall reaction was calculated to be favorable at -125.4 and -167.9 kJ/mol for $R = \text{Me}$, Ph , respectively.

We next considered the $R_2\text{NHC}\cdot\text{BH}_3$ adduct itself (Figure 3, Table 1), which has become a species of considerable interest, as have other carbene–hydridoborane adducts.^{44–56} The ring expansion product (**D**) is calculated to be 51.7 ($R = \text{Me}$) and 85.9 kJ/mol ($R = \text{Ph}$) lower in free energy than the adduct **A**. Importantly, this indicates that the $R_2\text{NHC}\cdot\text{BH}_3$ adduct is a kinetic rather than thermodynamic product. Modeling of the ring insertion pathway to form **D** gave a barrier for the first hydrogen migration of 167.1 ($R = \text{Me}$) and 149.3 kJ/mol ($R = \text{Ph}$), respectively, which is substantially higher than that calculated for the silanes and Rivard's borane. Overall this suggests that under more extreme conditions, or in the presence of other R groups on **B** that might stabilize the transition states, insertion of **B** into the C–N bond with concomitant hydride migration should be considered a possible outcome. Benchmarking calculations with a larger def2-QZVP basis set produced very similar relative energies, differing by at most 4.4 kJ/mol from the def2-TZVP results.

The primary point of difference between Rivard's borane and the BH_3 system is the presence of the lone pair bearing $-\text{NH}(\text{Dipp})$ group bound to boron in Rivard's system. The lone pair on the nitrogen has the potential to interact in a π -bonding fashion in circumstances where the boron center has only three σ bonds. Optimized geometries for the compounds along the reaction pathway for the simplified $-\text{NH}(\text{Me})$ substituted system are depicted in Figure 4, with bond distances and Wiberg bond indices (WBI) collated in Table 2.

Considering Me_2NHC , in the initial adduct **A** the B–N bond distance was calculated to be 1.522 Å. In **T1** this contracts to 1.438 Å and is further shortened to 1.387 Å in minimum **B**, consistent with substantial B–N double-bond character. The WBI value for the B–N bond in **B** was calculated to be 1.23 , and while this is substantially less than 2.00 , it is significantly greater than the WBI value of 0.86 for the B–N bond in **A**, which is clearly a single bond. For comparison, B–N single bonds are typically ca. 1.58 Å, while B–N double bonds are reported to be in the range 1.38 – 1.40 Å.^{57,58} The B–N benzene analogue borazine exhibits an intermediate bond distance of 1.44 Å.⁵⁹ Further evidence of a π interaction in the B–N bond can be found in the molecular orbitals (MOs) of the transition state **T1** (HOMO-2, Figure 5 (left)) and even more distinctly for minimum **B** (HOMO-3, Figure 5 (right)). From **B**, the B–N bond expands to 1.507 Å (WBI = 0.86) in minimum **C** and then contracts in **T3** (1.471 Å) with further contraction to 1.413 Å (WBI = 1.07) in the final product **D**, where it again gains some multiple-bond character. The B–N π interaction appears to have some effect in stabilizing transition

**Figure 5.** Plot of HOMO-2 for transition state **T1** (left) and HOMO-3 for minima **B** (right). **T1** and **B** are from reaction 2, Scheme 1.

states and minima relative to the BH_3 system. For **T1**, the barrier height is 45.1 kJ/mol lower for the $-\text{NH}(\text{Me})$ substituted borane in comparison with BH_3 , and similarly formation of the final products is preferentially favored by at least 70 kJ/mol. For minimum **C**, where boron has four σ bonds, the differences are lessened, with the BH_2NHMe system being 27.9 kJ/mol lower in energy than BH_3 .

As with our investigations with the silane system, we additionally investigated the reaction energetics for the analogous chloride (BCl_3). Examination of the relative energies of the adduct and the ring-expanded product (Table 1) indicates that with the chloride-substituted species the process is highly unfavorable, with an overall ΔG value of $+170$ kJ/mol. Moreover, we were unable to locate a transition state associated with the initial chloride migration (**T1**). These results can be rationalized by the relative bond dissociation energies (BDEs) for C–H (416 kJ/mol), B–H (330 kJ/mol), C–Cl (327 kJ/mol), and B–Cl (456 kJ/mol),^{60,61} from which it is clear that formation of C–H bonds is favored over the formation of C–Cl bonds (and breaking B–Cl bonds is more difficult than breaking B–H bonds), making the overall process more favorable for hydridoboranes, irrespective of possible kinetic barriers.

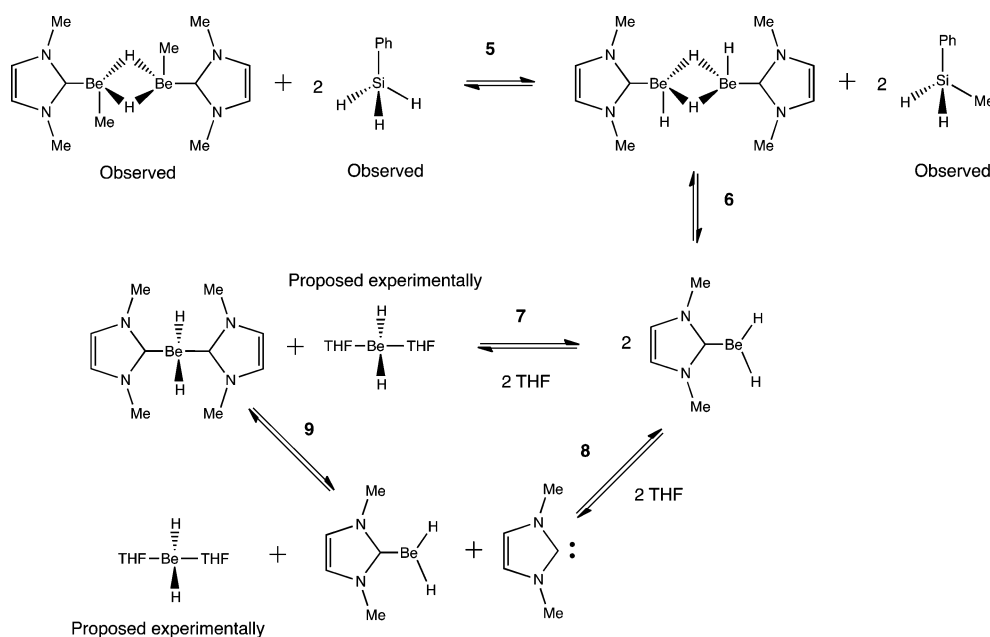
Beryllium Hydrides. For ring insertion of Be to occur with a mechanism analogous to that of the silane and borane requires the formation of a $R_2\text{NHC}\cdot\text{BeH}_2$ adduct, which was proposed as an intermediate in Hill's synthetic report ($R = \text{Dipp}$; reactions 3 and 4, Scheme 1).¹¹ The in situ formation of $R_2\text{NHC}\cdot\text{BeH}_2$ was postulated from the reaction of a methylated hydrido-bridged dimer and PhSiH_3 (the hydride source); heating at 80 °C for 6 h then gave the insertion product. Competitive insertion of the silane into the carbene C–N bond is not expected to occur under these conditions, as the silane reaction (reaction 1) required a higher temperature for several days. Indeed, the free energy (ΔG) for replacement of BeH_2 by either SiH_2Ph_2 or SiH_3Ph in the starting adduct (e.g.,

Table 3. SCS-MP2/def2-TZVP//M06-2X/def2-TZVP Calculated Free Energies (ΔG , kJ/mol) for the Reaction Mechanism of Beryllium Complexes To Form the Ring Insertion Product D^a

| reactants | | ΔG of reaction | | | | | | | |
|-----------------------|-------------------|------------------------|-----|----------|----------|----------|-------|----------|----------|
| | | reactants | A | T1 | B | T2 | C | T3 | D |
| Me ₂ NHC | BeH ₂ | 105.4 | 0.0 | 143.1 | 88.3 | 102.4 | −49.5 | 115.1 | −4.2 |
| 2 Me ₂ NHC | BeH ₂ | 135.6 | 0.0 | 67.2 | 24.2 | 53.8 | −34.1 | 9.0 | −115.9 |
| 2 Ph ₂ NHC | BeH ₂ | 153.8 | 0.0 | 75.5 | −2.6 | 39.0 | −43.1 | −17.0 | −185.0 |
| Me ₂ NHC | BeCl ₂ | 144.5 | 0.0 | <i>b</i> | 320.1 | 398.7 | 182.2 | <i>b</i> | 457.3 |
| 2 Me ₂ NHC | BeCl ₂ | 206.1 | 0.0 | <i>b</i> | <i>b</i> | <i>b</i> | 197.3 | <i>b</i> | <i>b</i> |

^aCompound A is the initial adduct between BeH₂ and R₂NHC. ^bNo transition state or minima located.

Scheme 2. Proposed Reaction Scheme Generating the Me₂NHC·BeH₂·Me₂NHC Starting Compound^a



^aCompounds observed or byproducts proposed by Hill and co-workers¹¹ experimentally are noted; in the synthetic report the NHC R groups were 2,6-diisopropylphenyl (Dipp) rather than methyl used in our model studies.

Me₂NHC·BeH₂ + SiH₃Ph → Me₂NHC·SiH₃Ph + BeH₂ for a simplified −Me substituted NHC) is calculated to be greater than +100 kJ/mol (MP2/def2-TZVP//M06-2X/6-31G(d)), which supports the expectation that competitive insertion of silane will not occur.

The formation of R₂NHC·BeH₂ as an intermediate was further supported by the observation that the insertion reaction also occurs in the absence of an external silane hydride source (reaction 4, Scheme 1) by using higher temperatures and a longer reaction time, with elimination of a THF adduct of Me₂Be, which would be expected to give R₂NHC·BeH₂ in situ.¹¹ The insertion/ring expansion product contains a second equivalent of R₂NHC, although the point of entry for the second R₂NHC is not immediately clear if the mechanism is indeed analogous to that of the silane and borane.

In essence there are two alternative pathways for the formation of the reported ring insertion product, which retains an R₂NHC bound to the Be atom. First, it is possible that the pathway is analogous to that of the silane and borane systems and starts with an R₂NHC·BeH₂ adduct, for which an additional free R₂NHC binds to the Be only after ring insertion. Alternatively, the additional R₂NHC could bind to

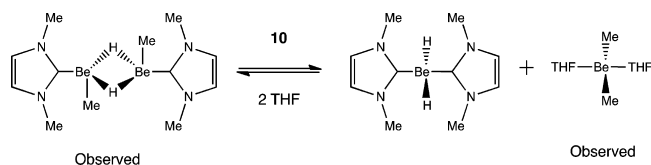
the BeH₂ before ring insertion, and the reaction proceeds from a molecule with an R₂NHC·BeH₂·R₂NHC framework.

We first modeled a BeH₂ insertion reaction pathway analogous to the pathway considered for the boranes and silanes, by considering only a single Me₂NHC ligand bound to BeH₂ and starting with an Me₂NHC·BeH₂ adduct (Table 3). The calculated ΔG value for the overall insertion reaction to form D in this case is only −4.2 kJ/mol. The barrier of the first hydrogen migration (T1) is very high at 143.1 kJ/mol, making the insertion unlikely from this compound under the reported conditions. Moreover, addition of a free NHC to the starting adduct NHC·BeH₂ to form NHC·BeH₂·NHC is favorable by 30.2 kJ/mol. Also of note, with R = Ph for the mono-R₂NHC adduct R₂NHC·BeH₂, locating a minimum energy structure presented significant problems, indicating this may not be a viable species. In contrast the adduct with two R₂NHC ligands bound to BeH₂ was well-behaved in silico. Hence, if free NHC is available, it is apparent that a mechanism whereby ring expansion/insertion occurs first followed by NHC ligation is unlikely.

We next considered a pathway which requires the formation of a bis-R₂NHC adduct of BeH₂ as the starting point for the ring insertion mechanism. No bis-R₂NHC adduct was observed

in the synthetic study of Hill and co-workers.¹¹ However, we hypothesize that $R_2NHC \cdot BeH_2 \cdot R_2NHC$ is the starting point for the insertion reaction either after reaction of the methylated bridged precursor with the silane (reaction 3, Scheme 1) or in the reaction under more extreme thermal conditions in the absence of the silane (reaction 4, Scheme 1). Proposed pathways for the formation of $Me_2NHC \cdot BeH_2 \cdot Me_2NHC$ are outlined in Schemes 2 and 3. These processes are consistent with the deuterium labeling experiments performed by Hill and co-workers.¹¹

Scheme 3. Reaction Generating $Me_2NHC \cdot BeH_2 \cdot Me_2NHC$ via Thermal Conditions (120 °C, 24 h)^a



^aCompounds observed by Hill and co-workers¹¹ are noted; in the synthetic report the NHC R groups were 2,6-diisopropylphenyl (Dipp) rather than methyl used in our model studies.

We calculated ΔG of these pathways using a model system of Me_2NHC in place of the $Dipp_2NHC$ ($Dipp = 2,6$ -diisopropylphenyl) utilized in the synthetic report. In both cases, the generation of $Me_2NHC \cdot BeH_2$ or $Me_2NHC \cdot BeH_2 \cdot Me_2NHC$ from the hydrido-bridged starting material is energetically unfavorable, which is consistent with Hill's indication that these intermediates were not observed.

In the case where silane was used as a hydride source (Scheme 2), the initial metathesis reaction (reaction 5) is calculated to be favorable with $\Delta G = -24.7$ kJ/mol. Splitting this species into two $Me_2NHC \cdot BeH_2$ molecules (reaction 6) is unfavorable by 82.5 kJ/mol. An unidentified beryllium

byproduct observed in the synthetic study was suggested to be a THF adduct of BeH_2 on the basis of NMR spectra.¹¹ Generation of this byproduct from 2 equiv of $Me_2NHC \cdot BeH_2$ giving $THF \cdot BeH_2 \cdot THF$ and our required $Me_2NHC \cdot BeH_2 \cdot Me_2NHC$ molecule is calculated to be unfavorable by 33.4 kJ/mol (reaction 7). If the reaction is considered as stepwise as possible (reactions 8 and 9), the elimination of $THF \cdot BeH_2 \cdot THF$ gives one remaining $Me_2NHC \cdot BeH_2$ and a free Me_2NHC and is unfavorable by 63.5 kJ/mol (reaction 8). From here, the combination of $Me_2NHC \cdot BeH_2$ and Me_2NHC , forming $Me_2NHC \cdot BeH_2 \cdot Me_2NHC$, is favorable by 30.1 kJ/mol (reaction 9). Despite the unfavorable pathway leading to the required starting material (overall ΔG for reactions 5–7 +91.2 kJ/mol), the larger negative ΔG for the insertion (-115.9 kJ/mol; Table 3) gives an overall favorable ΔG for the entire process from the methyl hydrido bridged species and $PhSiH_3$.

In the case where no silane is added (reaction 4) and the reaction proceeds under thermal conditions from the methyl hydrido bridged species, generation of $Me_2NHC \cdot BeH_2 \cdot Me_2NHC$ and the experimentally observed $THF \cdot BeH_2 \cdot THF$ is calculated to be unfavorable by 105.6 kJ/mol (Scheme 3, reaction 10), but again the onward insertion reaction with $\Delta G = -115.9$ kJ/mol (Table 3) results in an overall favorable transformation to the observed insertion product (D).

While these proposed pathways are speculative, they are consistent with experimental observations. In this regard there is reasonable justification for considering $R_2NHC \cdot BeH_2 \cdot R_2NHC$ as the starting point for the ring insertion mechanism.

Subsequently, we investigated the insertion pathway using $R_2NHC \cdot BeH_2 \cdot R_2NHC$ as a starting complex for $R = Me, Ph$ (Figure 6). Addition of a second equivalent of R_2NHC to $R_2NHC \cdot BeH_2$ was calculated to be favorable by 30.2 and 48.4 kJ/mol for $R = Me, Ph$, respectively. With $R_2NHC \cdot BeH_2 \cdot R_2NHC$, the barrier for the first hydride migration (T1) is 67.2 (R = Me) and 75.5 kJ/mol (R = Ph), which is significantly less than in the case with the monoadduct $Me_2NHC \cdot BeH_2$. For

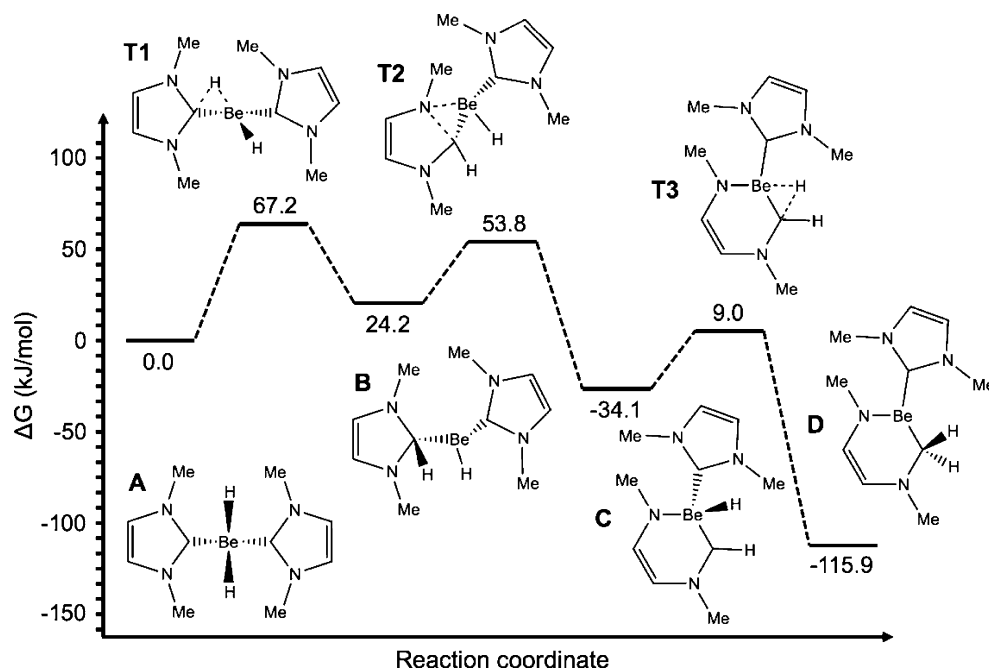


Figure 6. Free energy reaction profile (ΔG , kJ/mol) for insertion of Be into the NHC C–N bond from $NHC \cdot BeH_2 \cdot NHC$ calculated with SCS-MP2/def2-TZVP//M06-2X/def2-TZVP. Formal charges are omitted. Minima are denoted A–D, and transition states are denoted T n ($n = 1–3$).

$R_2NHC \cdot BeH_2 \cdot R_2NHC$ ΔG for the overall insertion reaction from **A** is calculated to be -115.9 ($R = Me$) and -185.0 ($R = Ph$) kJ/mol.

The final product (**D**) contains a rare example of a Be–N π interaction. The optimized Be–N bond distance in the final product **D** is 1.558 \AA (cf. the experimental report, 1.587 \AA),¹¹ which is substantially reduced from the 1.709 \AA for the Be–N bond in the intermediate **C**. The Be–N bond distance in **D** is consistent with the very few other reports of Be–N π bonding ($1.52\text{--}1.57 \text{ \AA}$).^{62,63} A π interaction is apparent in the HOMO-1 for **D** (Figure 7). While the WBI values for the Be–N bonds in

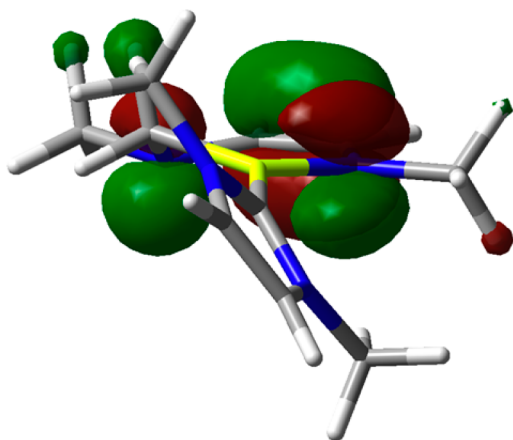


Figure 7. HOMO-1 for the BeH_2 insertion product (compound **D**, Figure 6), viewed in the plane of the expanded Me_2NHC ring.

compounds **C** and **D** are both less than 1 (0.40 in **C**, 0.57 in **D**), WBI values are poorly estimated in organometallic s-block complexes due to the substantial ionic character of the bonds^{64,65} and a clear increase is calculated from **C** to **D**. We therefore suggest that Hill's compound **D** represents an extremely rare case of a Be–N π interaction, albeit not a full double bond.

Another point of difference from the silane and borane analogues is the solvent. For B and Si, the reactions took place in the weakly interacting solvent toluene. Our calculations on these systems incorporating a toluene solvent model produced only subtle differences from gas-phase calculations for the neutral compounds under consideration. However, the Be reaction occurred in THF. While use of a THF solvent model did not substantially affect the energies in test calculations, formation of distinct molecular interactions between the Be centers and THF is a possibility and could strongly affect at what point the “second” carbene is introduced. We investigated this possibility using $Me_2NHC \cdot BeH_2$ as the starting point of the mechanism, for which the first hydrogen atom migration results in a species containing a two-coordinate Be structure and a high barrier (143.1 kJ/mol). A single THF was added to Be to produce a $Me_2NHC \cdot BeH_2 \cdot THF$ species, from which the transition state for hydrogen migration to the NHC carbene carbon was investigated. The barrier was calculated to be 91.2 kJ/mol , which is lower than the case without the explicit THF, but it remains significantly higher than the corresponding bis- Me_2NHC complex (67.2 kJ/mol). Calculation of this barrier in $R_2NHC \cdot BeH_2 \cdot THF$ using the full 2,6-diisopropylphenyl (Dipp) substituted NHC gave a similar value of 97.7 kJ/mol . The ΔG for the reaction $Me_2NHC \cdot BeH_2 \cdot THF + Me_2NHC \rightarrow Me_2NHC \cdot BeH_2 \cdot Me_2NHC + THF$ is calculated to be -44.8

kJ/mol, which suggests that if any free NHC is present, that the required bis- Me_2NHC complex will readily be formed. Additionally, the calculated ΔG for the addition of one THF to $Me_2NHC \cdot BeH_2$ is unfavorable by 14.7 kJ/mol , whereas addition of the second R_2NHC is favorable by 30.1 and 48.4 kJ/mol for $R = \text{methyl, phenyl}$, respectively, as discussed above. Again, these results suggest that it is more likely that the “second” NHC is incorporated prior to insertion and that the $R_2NHC \cdot BeH_2 \cdot R_2NHC$ adduct may be considered a reasonable starting point.

As in the other analogous cases studied (Si, B), when using $R_2NHC \cdot BeCl_2$ or $R_2NHC \cdot BeCl_2 \cdot R_2NHC$ as the starting compound, a similar ring expansion is calculated to be highly unfavorable (457 kJ/mol for $Me_2NHC \cdot BeCl_2$), and for several species no stable minima or transition states could even be located. The adducts for this species are also highly stabilized, for example by 206 kJ/mol for $Me_2NHC \cdot BeCl_2 \cdot Me_2NHC$.

CONCLUSIONS

Our findings here on the mechanism for the insertion/ring expansion of N-heterocyclic carbenes in reactions with boranes and beryllium hydrides are generally consistent with the mechanism previously determined for the same reaction with silanes (with the exception of the beryllium hydride requiring a second NHC ligand). The ring-insertion mechanism follows three steps: (1) hydrogen atom migration from the hydride source to the carbene carbon, (2) C–N bond expansion of the NHC with insertion of B or Be into the ring, and (3) migration of the second H atom from B or Be to the carbene carbon. The mechanism is unfavorable for analogous chloride systems. Of particular interest here is our finding that $NHC \cdot BH_3$ adducts are thermodynamically unstable with respect to this transformation, which might be considered in the future use of this adduct, particularly under conditions of heating or, for example, microwave.

ASSOCIATED CONTENT

Supporting Information

Tables and figures giving Cartesian coordinates and electronic energies for all species calculated and energy profiles for insertion reactions involving derivatives from tables not featured in the paper. This material is available free of charge via the Internet at <http://pubs.acs.org>.

AUTHOR INFORMATION

Corresponding Authors

*E-mail for D.J.D.W.: david.wilson@latrobe.edu.au.

*E-mail for J.L.D.: j.dutton@latrobe.edu.au.

Notes

The authors declare no competing financial interest.

ACKNOWLEDGMENTS

We thank the La Trobe Institute for Molecular Sciences and La Trobe University for their generous funding of this work. Grants of computing resources from the VPAC and NCI-NF are acknowledged. This work was also supported by an ARC DECRA fellowship (J.L.D., DE130100186). Finally, we thank C. Boddicker for useful discussions.

REFERENCES

- (1) Al-Rafia, S. M. I.; Malcolm, A. C.; Liew, S. K.; Ferguson, M. J.; Rivard, E. J. *Am. Chem. Soc.* **2011**, *133*, 777.

- (2) Al-Rafia, S. M. I.; Malcolm, A. C.; McDonald, R.; Ferguson, M. J.; Rivard, E. *Angew. Chem., Int. Ed.* **2011**, *50*, 8354.
- (3) Al-Rafia, S. M. I.; Malcolm, A. C.; McDonald, R.; Ferguson, M. J.; Rivard, E. *Chem. Commun.* **2012**, *48*, 1308.
- (4) Thimer, K. C.; Al-Rafia, S. M. I.; Ferguson, M. J.; McDonald, R.; Rivard, E. *Chem. Commun.* **2009**, *45*, 7119.
- (5) Wang, Y.; Quillian, B.; Wei, P.; Wannere, C. S.; Xie, Y.; King, R. B.; Schaefer, H. F., III; Schleyer, P. v. R.; Robinson, G. H. *J. Am. Chem. Soc.* **2007**, *129*, 12412.
- (6) Francis, M. D.; Hibbs, D. E.; Hursthouse, M. B.; Jones, C.; Smithies, N. A. *J. Chem. Soc., Dalton Trans.* **1998**, *27*, 3249.
- (7) Alexander, S. G.; Cole, M. L.; Furfari, S. K.; Kloth, M. *Dalton Trans.* **2009**, 2909.
- (8) Abraham, M. Y.; Wang, Y.; Xie, Y.; Wei, P.; Schaefer, H. F., III; Schleyer, P. v. R.; Robinson, G. H. *J. Am. Chem. Soc.* **2011**, *133*, 8874.
- (9) Ghadwal, R. S.; Azhakar, R.; Roesky, H. W.; Propper, K.; Ditttrich, B.; Goedecke, C.; Frenking, G. *Chem. Commun.* **2012**, *48*, 8166.
- (10) Al-Rafia, S. M. I.; McDonald, R.; Ferguson, M. J.; Rivard, E. *Chem. Eur. J.* **2012**, *18*, 13810.
- (11) Arrowsmith, M.; Hill, M. S.; Kociok-Köhn, G.; MacDougall, D. J.; Mahon, M. F. *Angew. Chem., Int. Ed.* **2012**, *51*, 2098.
- (12) Schmidt, D.; Berthel, J. H. J.; Pietsch, S.; Radius, U. *Angew. Chem., Int. Ed.* **2012**, *51*, 8881.
- (13) Frey, G. D.; Lavallo, V.; Donnadiou, B.; Schoeller, W. W.; Bertrand, G. *Science* **2007**, *316*, 439.
- (14) Masuda, J. D.; Schoeller, W. W.; Donnadiou, B.; Bertrand, G. *Angew. Chem., Int. Ed.* **2007**, *46*, 7052.
- (15) Frey, G. D.; Masuda, J. D.; Donnadiou, B.; Bertrand, G. *Angew. Chem., Int. Ed.* **2010**, *49*, 9444.
- (16) Iversen, K. J.; Wilson, D. J. D.; Dutton, J. L. *Dalton Trans.* **2013**, *42*, 11035.
- (17) Wang, Y.; Xie, Y.; Wei, P.; King, R. B.; Schaefer, H. F., III; Schleyer, P. v. R.; Robinson, G. H. *Science* **2008**, *321*, 1069.
- (18) Wilson, D. J. D.; Couchman, S.; Dutton, J. L. *Inorg. Chem.* **2012**, *51*, 7657.
- (19) Ghadwal, R. S.; Roesky, H. W.; Merkel, S.; Henn, J.; Stalke, D. *Angew. Chem., Int. Ed.* **2009**, *48*, 5683.
- (20) Filippou, A. C.; Chernov, O.; Schnakenburg, G. *Angew. Chem., Int. Ed.* **2009**, *48*, 5687.
- (21) Brahmi, M. M.; Monot, J.; Murr, M. D.; Curran, D. P.; Fensterbank, L.; Lacôte, E.; Malacria, M. *J. Org. Chem.* **2010**, *75*, 6983.
- (22) Solov'yev, A.; Ueng, S.; Monot, J.; Fensterbank, L.; Malacria, M.; Lacôte, E.; Curran, D. P. *Org. Lett.* **2010**, *12*, 2998.
- (23) Tsai, J.; Lin, S.; Yang, R. B.; Yap, G. P. A.; Ong, T. *Organometallics* **2010**, *29*, 4004.
- (24) Wang, Y.; Xie, Y.; Abraham, M. Y.; Wei, P.; Schaefer, H. F., III; Schleyer, P. v. R.; Robinson, G. H. *Organometallics* **2011**, *30*, 1303.
- (25) Bissinger, P.; Braunschweig, H.; Kupfer, T.; Radacki, K. *Organometallics* **2010**, *29*, 3987.
- (26) Ramnial, T.; Jong, H.; McKenzie, I. D.; Jennings, M.; Clyburne, J. A. C. *Chem. Commun.* **2003**, *39*, 1722.
- (27) Zlatogorsky, S.; Ingleson, M. J. *Dalton Trans.* **2012**, *41*, 2685.
- (28) Jana, A.; Azhakar, R.; Tavcar, G.; Roesky, H. W.; Objartel, I.; Stalke, D. *Eur. J. Inorg. Chem.* **2011**, *2011*, 3686.
- (29) Pan, X.; Lacôte, E.; Lalevee, J.; Curran, D. P. *J. Am. Chem. Soc.* **2012**, *134*, 5669.
- (30) Horn, M.; Mayr, H.; Lacôte, E.; Merling, E.; Deaner, J.; Wells, S.; McFadden, T.; Curran, D. P. *Org. Lett.* **2012**, *14*, 82.
- (31) Curran, D. P.; Solov'yev, A.; Brahmi, M. M.; Fensterbank, L.; Malacria, M.; Lacôte, E. *Angew. Chem., Int. Ed.* **2011**, *50*, 10294.
- (32) Frisch, M. J.; Trucks, G. W.; Schlegel, H. B.; Scuseria, G. E.; Robb, M. A.; Cheeseman, J. R.; Scalmani, G.; Barone, V.; Mennucci, B.; Petersson, G. A.; Nakatsuji, H.; Caricato, M.; Li, X.; Hratchian, H. P.; Izmaylov, A. F.; Bloino, J.; Zheng, G.; Sonnenberg, J. L.; Hada, M.; Ehara, M.; Toyota, K.; Fukuda, R.; Hasegawa, J.; Ishida, M.; Nakajima, T.; Honda, Y.; Kitao, O.; Nakai, H.; Vreven, T.; Montgomery, J. A., Jr.; Peralta, J. E.; Ogliaro, F.; Bearpark, M.; Heyd, J. J.; Brothers, E.; Kudin, K. N.; Staroverov, V. N.; Keith, T.; Kobayashi, R.; Normand, J.; Raghavachari, K.; Rendell, A.; Burant, J. C.; Iyengar, S. S.; Tomasi, J.; Cossi, M.; Rega, N.; Millam, J. M.; Klene, M.; Knox, J. E.; Cross, J. B.; Bakken, V.; Adamo, C.; Jaramillo, J.; Gomperts, R.; Stratmann, R. E.; Yazyev, O.; Austin, A. J.; Cammi, R.; Pomelli, C.; Ochterski, J. W.; Martin, R. L.; Morokuma, K.; Zakrzewski, V. G.; Voth, G. A.; Salvador, P.; Dannenberg, J. J.; Dapprich, S.; Daniels, A. D.; Farkas, Ö.; Foresman, J. B.; Ortiz, J. V.; Cioslowski, J.; Fox, D. J. *Gaussian 09, Revision D.01 ed.*; Gaussian, Inc., Wallingford, CT, 2009.
- (33) Zhao, Y.; Truhlar, D. G. *Theor. Chem. Acc.* **2008**, *120*, 215.
- (34) Becke, A. D. *Phys. Rev. A* **1988**, *38*, 3098.
- (35) Ernzerhof, M.; Perdew, J. P. *J. Chem. Phys.* **1998**, *109*, 3313.
- (36) Schäfer, A.; Horn, H.; Ahlrichs, R. *J. Chem. Phys.* **1992**, *97*, 2571.
- (37) Schäfer, A.; Huber, C.; Ahlrichs, R. *J. Chem. Phys.* **1994**, *100*, 5829.
- (38) Peng, C.; Ayala, P. Y.; Schlegel, H. B.; Frisch, M. J. *J. Comput. Chem.* **1996**, *17*, 49.
- (39) Gerenkamp, M.; Grimme, S. *Chem. Phys. Lett.* **2004**, *392*, 229.
- (40) Jung, Y.; Lochan, R. C.; Dutoi, A. D.; Head-Gordon, M. *J. Chem. Phys.* **2004**, *121*, 9793.
- (41) Pomelli, C.; Tomasi, J.; Barone, V. *Theor. Chim. Acta* **2001**, *105*, 446.
- (42) Cancès, E.; Mennucci, B.; Tomasi, J. *J. Chem. Phys.* **1997**, *107*, 3032.
- (43) Tomasi, J.; Mennucci, B.; Cancès, E. *J. Mol. Struct. (THEOCHEM)* **1999**, *464*, 211.
- (44) Curran, D. P.; Boussonniere, A.; Geib, S. J.; Lacôte, E. *Angew. Chem., Int. Ed.* **2012**, *51*, 1602.
- (45) Merling, E.; Lamm, V.; Geib, S. J.; Lacôte, E.; Curran, D. P. *Org. Lett.* **2012**, *14*, 2690.
- (46) Tang, C. Y.; Thompson, A. L.; Aldridge, S. J. *Am. Chem. Soc.* **2010**, *132*, 10578.
- (47) Tang, C. Y.; Smith, W.; Thompson, A. L.; Vidovic, D.; Aldridge, S. *Angew. Chem., Int. Ed.* **2011**, *50*, 1359.
- (48) Monot, J.; Solov'yev, A.; Bonin-Dubarle, H.; Derat, E.; Curran, D. P.; Robert, M.; Fensterbank, L.; Malacria, M.; Lacôte, E. *Angew. Chem., Int. Ed.* **2010**, *49*, 9166.
- (49) Ines, B.; Patil, M.; Carreras, J.; Goddard, R.; Thiel, W.; Alcarazo, M. *Angew. Chem., Int. Ed.* **2011**, *50*, 8400.
- (50) Bissinger, P.; Braunschweig, H.; Kraft, K.; Kupfer, T. *Angew. Chem., Int. Ed.* **2011**, *50*, 4704.
- (51) Ueng, S.; Solov'yev, A.; Yuan, X.; Geib, S. J.; Fensterbank, L.; Lacôte, E.; Malacria, M.; Newcomb, M.; Walton, J. C.; Curran, D. P. *J. Am. Chem. Soc.* **2009**, *131*, 11256.
- (52) Solov'yev, A.; Geib, S. J.; Lacôte, E.; Curran, D. P. *Organometallics* **2012**, *31*, 54.
- (53) Wang, Y.; Quillian, B.; Wei, P.; Xie, Y.; Wannere, C. S.; King, R. B.; Schaefer, H. F., III; Schleyer, P. v. R.; Robinson, G. H. *J. Am. Chem. Soc.* **2008**, *130*, 3298.
- (54) Casely, I. J.; Liddle, S. T.; Blake, A. J.; Wilson, C.; Arnold, P. L. *Chem. Commun.* **2007**, 5037.
- (55) Kinjo, R.; Donnadiou, B.; Celik, M. A.; Frenking, G.; Bertrand, G. *Science* **2011**, *333*, 610.
- (56) Li, X.; Curran, D. P. *J. Am. Chem. Soc.* **2013**, *135*, 12076.
- (57) Paetzold, P. *Pure Appl. Chem.* **1991**, *63*, 345.
- (58) Clippard, F. B.; Bartell, L. S. *Inorg. Chem.* **1970**, *9*, 2439.
- (59) Miessler, G. L.; Fisher, P. J.; Tarr, D. A. *Inorganic Chemistry*, 5th ed.; Pearson: Boston, 2014.
- (60) Cotton, F. A.; Wilkinson, G. *Advanced Inorganic Chemistry*, 5th ed.; Wiley: New York, 1988.
- (61) Dean, J. A. *Lange's Handbook of Chemistry*, 15th ed.; McGraw-Hill: New York, 1999.
- (62) Niemeyer, M.; Power, P. P. *Inorg. Chem.* **1997**, *36*, 4688.
- (63) Atwood, J. L.; Stucky, G. D. *J. Am. Chem. Soc.* **1969**, *91*, 4426.
- (64) Cuevas, G.; Juaristi, E. *J. Am. Chem. Soc.* **1997**, *119*, 7545.
- (65) Couchman, S.; Holzmann, N.; Frenking, G.; Wilson, D. J. D.; Dutton, J. L. *Dalton Trans.* **2013**, *42*, 11375.